Journal of Translational Medicine

RESEARCH

Open Access

# SULT2B1: a novel therapeutic target in colorectal cancer via modulation of AKT/PKM2-mediated glycolysis and proliferation

Jianxing Ma[1], Fengyao Sun[2], Wen Li[2], Ruihang Du[2], Mingchan Liu[2], Qiuya Wei[1], Boxiong Kang[1], Siyuan Yan[2*] and Chen Wang[1*]

## Abstract

**Background** Sulfotransferase family 2B member 1 (SULT2B1) is involved in regulating cell proliferation, migration and metabolism. However, there is still dispute regarding whether SULT2B1 acts as an oncogene or a suppressor, and the intrinsic mechanisms in modulating tumor progression need to be further elucidated.

**Methods** This work aims to reveal the relationship among SULT2B1, AKT, PKM2 signaling and glycolytic pathways, and provided a theoretical basis for SULT2B1 as a potential therapeutic target for CRC.Bioinformatics methods, immunohistochemistry (IHC) and immunoblotting assays were performed to analyze the correlation between SULT2B1 and colorectal cancer (CRC). The effect of SULT2B1 on cell proliferation and migration were investigated by several phenotypic experiments in vitro and animal studies. The SULT2B1 interacting proteins were determined by immunofluorescence, immunoprecipitation and GST-pull down assays. Immunoblotting and mCherry-GFP-LC3 assays were performed to analysis autophagy. Chromatin immunoprecipitation (CHIP) assay was utilized to detect the effect of SULT2B1 in regulating transcription. Small molecule agonist/antagonist was used to modify protein activity and therefore analyze the mutual relationships.

**Results** SULT2B1 is a predictive biomarker that is abnormally overexpressed in CRC tissues. Overexpression of SULT2B1 promoted cell proliferation and migration, while its knockout suppressed these processes. Furthermore, SULT2B1 could directly interact with the oncogene AKT and thereby enhance the activity of AKT-mTORC1 signaling. Furthermore, PKM2 was found to bind with SULT2B1, and regulated by SULT2B1 at both transcription and degradation levels. Moreover, blocking glycolysis attenuated the promoting effect of OE-SULT2B1.

**Conclusion** SULT2B1 acts as an oncogene in CRC via modulating the AKT/PKM2 axis, therefore making it a promising diagnostic and therapeutic target for CRC.

**Keywords** SULT2B1, Colorectal cancer, Cell proliferation, AKT signaling pathway, PKM2

## Introduction

Colorectal cancer (CRC) possesses high morbidity and mortality rate worldwide, with approximately 1.9 million new cases and 0.9 million deaths annually, making it an enormous burden on society [1]. The diagnosis stage impacts therapeutic effectiveness and survival rate, however, the majority of patients are already in the middle or advanced stage when they are diagnosed due to the concealment characteristics of CRC [2]. Thus,

*Correspondence:
Siyuan Yan
yansy@mail.jnmc.edu.cn
Chen Wang
chenwang@lzu.edn.cn
[1] Department of General Surgery, The Second Hospital & Clinical Medical School, Lanzhou University, Lanzhou 730000, China
[2] Precision Medicine Laboratory for Chronic Non-Communicable Diseases of Shandong Province, Institute of Precision Medicine, Jining Medical University, Jining 272067, China

early diagnosis and precision treatment are crucial and vital, emphasizing the importance of identifying better biomarkers for diagnosis and targeted therapy [3].

Sulfotransferase family 2B member 1 (*SULT2B1*), located at chromosomal loci 19q13.3, plays a role in controlling the metabolism of cholesterol and hydroxysteroid [4, 5]. Previous research indicates that SULT2B1 plays crucial roles in regulating immunological responses, such as suppressing the LXR pathway to impact the immunity checkpoint [6], alleviating ulcerative colitis, limiting neutrophil recruitment and gut inflammation, and promoting pro-inflammatory macrophage polarization [7–9]. Moreover, it has also been associated with the progression of numerous cancer types, including prostate cancer, gastric cancer, hepatocellular carcinoma, and CRC [10–12]. Besides playing a role in regulating cell proliferation, SULT2B1 also enhances cell invasion and radio-resistance in CRC [13]. Little is known about the association between SULT2B1 and the glycolytic pathway, except that knocking down SULT2B1 weakened glycolytic metabolism in LoVo cells [14]. Here, we validated that it has the potential to modify the glycolytic pathway by promoting and interacting with PKM2 (Pyruvate Kinase M2), a rate-limiting enzyme in the glycolytic pathway.

As a serine/threonine kinase, also known as protein kinase B, AKT plays pivotal roles in a variety of physiological and pathological processes [15]. A wide range of growth signals and biochemical mechanisms can activate AKT, followed by regulating the function of various downstream proteins involved in cellular proliferation, invasion, migration, and metabolism [16]. An important downstream signaling molecule is mTOR (the mammalian target of rapamycin), which could influence transcription and translation by its two downstream effectors [17]. In mammalian cells, three highly homologous AKT isoforms (AKT1, AKT2 and AKT3) are expressed and perform analogous functions, yet studies showed AKT isoforms display opposite functions in tumor initiation and growth [18]. Meanwhile, the expressions of AKT isoforms have tissue and cell specificity. As one of the rate-limiting enzymes in glycolysis, pyruvate kinase catalyzes the conversion of phosphoenolpyruvate to pyruvate, while PKM2 is essential for aerobic glycolysis in cancer cells [19]. Apart from glycolysis, PKM2 participates in regulating cancer cell proliferation, invasion and metastasis [20]. Despite some controversy, there have been studies revealing the relationship between AKT and PKM2, as they may accompany or promote each other in certain circumstances [21, 22]. In the current study, we verified that AKT functions upstream of PKM2 in the SULT2B1-modified CRC cells.

In this study, we demonstrated that SULT2B1 was abundantly expressed in CRC and positively regulated cell proliferation in vitro and in vivo. Moreover, SULT2B1 positively modified the protein levels of AKT and PKM2, and interacted with both of them. Further investigation indicated that SULT2B1 regulates CRC progression in an AKT/PKM2-dependent manner, and therefore uncovering an intimate relationship between SULT2B1 and AKT/PKM2 signaling, which could shed light on the diagnosis and therapy for CRC.

## Materials and methods

### Chemicals and antibodies

Cells RIPA lysis and extraction buffer (89901) were purchased from Thermo Scientific (Waltham, MA, 02454). PMS (P9625) and MTS (G111) were obtained from Sigma-Aldrich and Promega Corporation (Madison, WI, USA), respectively. Modified Giemsa staining solution (C0131), Crystal violet staining solution (C0121), ECL luminescent solution (P0018S), EDU cell proliferation kit with Alexa Fluor594 (C0078S) and Eosin Staining Solution (C0109) were obtained from Beyotime (Shanghai, China). Cell Cycle Detection Kit (KGA512) was purchased from Key Gene (Netherlands). SC79 (HY-18749), API-2 (HY-15457), Shikonin (HY-N0822), and Tepp46 (HY-18657) were all purchased from MedChemexpress (NJ, USA). 2DG (PHR9231) and Chloroquine diphosphate salt (C6628, CQ) was obtained from Sigma (USA). The detailed information of antibodies was shown in Table S1.

### Cell cultivations and transfections

The CRC cell lines including HT29, SW480, HCT116, HCT8, and LOVO were obtained from ATCC. All the cells were cultured in Dulbecco's modified Eagle's medium (DMEM) (C11995500BT, GIBCO, NY, USA) complemented with 10% bovine serum (10099-141, GIBCO, NY, USA) and 1% antibiotics (UB89609, BIOODIN, China) at 37 °C,5% $CO_2$. When the cells grew to 70%–80% confluency, transfections were performed. For the OE-SULT2B1 cell line construction, the OE-Ctrl and OE-SULT2B1 plasmids bought from Fenghui Biotechnology (China) were transfected by Attractive Transfection Reagent (301005, QIAGEN, Germany) according to the manufactory' instructions, and the transfection was conducted in a 6 cm dish with 1000 ng plasmids. For SULT2B1 knockout cell line generation, the KO-SULT2B1 plasmids (1000 ng) (Genai Biotechnology) were transfected in a 6 cm dish by Attractive Transfection Reagent, and then monoclonal cells were screened and validated. The sequences of KO-SULT2B1 Crisprcas9 gRNA were as follows (gRNA: GATGGGCACGGA GCGGATCCAGG). For interfering the AKT expression

level, the siRNA (25 nM final concentration) (sc-43609, Santa, USA) were transfected by DharmaFECT Transfection Reagent (T-2002-02, Thermo Fisher Scientific, USA) according to the manufactory' instructions. Moreover, theOE-PKM2 lentivirus (used at 100 MOI) was bought from OBiO (H5809, Shanghai, China), and infected indicated cells for 24 h.

#### Immunoblotting

The whole protein lysates were extracted from indicated cells, CRC patient's tissues and mouse tissues with RIPA lysis and denatured at 100℃ for 15 min. Then the samples were separated by Pre-SDS-PAGE (Gel42012, E-life technology Beijing), transferred to PVDF membranes (88520, Invitrogen, USA), and blocked with 5% skim milk powder. Whereafter, the membranes were incubated with the specific primary antibody at 4℃ overnight, the secondary antibody for 1 h at room temperature, and the bands were visualized by means of the ECL luminescent solution.

The surgical specimens of CRC patients were collected from the department of general surgery at the Second Hospital of Lanzhou University, and the detailed information of CRC surgical patients was listed in Table S2.

#### Real-time quantity PCR

The total cellular RNA was extracted using the RNA Easy Fast Tissue/Cell Kit (DP451, TIANGEN, Beijing, China) according to the manufacturer's protocol. 1 ug of RNA was conducted as reverse transcription incubated at 37 ℃ for 15 min using 5 × EasyQuickMasterMix (CW2634M, CWBIO, China). The reactions were terminated by heat inactivation at 85 °C for 5 s. Subsequently, qPCR was initiated with a degeneration for 10 min and then went into the cycle program with 95 °C (15 s), 60 °C (45 s), and 72 °C (1 min) for up to 40 cycles. The sequences of primers for amplification were as follows:

| Gene | Primer | Nucleotides |
|---|---|---|
| SULT2B1 | Forward (5′ → 3′) Reverse (5′ → 3′) | CGGGCTTGTGGG ACACCTA CATCTT GGGTGTTCTCCGCC |
| β-Actin | Forward (5′ → 3′) Reverse (5′ → 3′) | GCCTGACGGCCA GGTCATCAC CGG ATGTCCACGTCA CACTTC |

#### Cell viability assay

The specific cells were divided into 96-well plates (5000–10,000 cells per well) and cultured overnight with or without specific treatments. Whereafter, the detection mix containing MTS/PMS (20:1) was added with 10 μL per well, and continuously cultured for 1–2 h. Cell viability were detected at 492 nm absorbance by a microplate reader.

#### Colony growth assay and EDU-staining cell proliferation assay

For colony growth assay, the cells were separated into 12-well plates, ensuring 100–200 cells per well, and continually cultured for approximately 14 days. After that, the cell colonies were fixed with paraformaldehyde at room temperature for 15 min, stained with Giemsa dye, and then pictures were taken, followed by counting the number of colonies by means of Image J software.

For EDU-staining cell proliferation assay, the cells were separated into a 24-well plate and cultured continuously overnight. Subsequently, EDU staining was performed as the manufacturer's introduction. Finally, the photographs were taken under a fluorescence microscope, and the data was analyzed using Photoshop and Image J software.

#### Would healing test and transwell invasion assay

For a wound healing test, the cells with 70–80% confluence were collected, suspended, and divided into scratch plugs in a 12-well plate, with 110 μL per small compartment. After growing for an entire night, the plugins were vertically removed, and floating cells were washed away with PBS. Following this, low serum medium (1% FBS, 1% antibiotics) was added to each well. Then the cells were cultured continuously with or without specific treatment. At indicated time, a microscope was used to photograph the scratch statuses and measure the closed wound areas with Photoshop software.

For Transwell invasion assay, in brief, the cells suspended by the low serum glucose-free DMEM medium (1%) were separated into the up chamber with Matrigel following the 10% serum high glucose DMEM medium was added to the lower chamber. After a 24–48 h continuous culture, the cells were fixed, washed, and stained. Whereafter, the images were taken under a microscope, and then counted by Image J software.

#### Immunohistochemistry (IHC) staining

The human tissue microarray (D100Co01) was purchased from Ernan Biotechnological Company (Xi'an, China). For xenograft tumors, the samples were fixed, dehydrated, embedded in paraffin, and then sectioned into sections with a thickness of 4 μm. Subsequently, the microarray and sections were baked, dewaxed, hydrated and repaired antigen. Thereafter, the Rabbit/mouse IgG-two-step immunohistochemistry kit (SV0004, BOSTER) was used following the instructions (primary antibody: diluted at 1:100). After DAB (AR1027-3, BOSTER) color developing, hematoxylin staining, dehydrating and sealing sheet, scanning was performed by 3D HISTECH.

The IHC results were scored by the product between the percentage of positive cells (1, 2, 3 and 4 represent 0–25%, 26–50%, 51–75%, 76–100%, respectively) and the intensity (1, 2 and 3 represent low, moderate, high, respectively).

#### Co-immunoprecipitation assay

The cells were lysed by IP lysis buffer (P0013, Beyotime), and the specific primary antibodies were added into the lysates for incubation at 4 ℃ overnight. After that, the proteins were precipitated by Protein A/G magnetic beads (MCE: HY-K0202; NJ, USA) via a hopper magnet. Then the proteins were separated with heating, and then the samples were subjected to immunoblotting analysis.

#### GST pull-down assay

The purified proteins of His-SULT2B1 (HY-P74420) as well as His-AKT-GST (HY-P76666) were purchased from MCE (NJ, USA), and they were dissolved by water. Whereafter, 10 ug of the purified proteins were incubated at 4 ℃ for 4–6 h, and the GST magnetic agarose beads (P2258, Beyotime), with a magnetic stand, were added to precipitate the proteins. With a heat at 100 ℃ for 10 min, the proteins were separated from the beads, and then the samples were electrophoresed in SDS-PAGE, and subjected to immunoblotting analysis.

#### Immunofluorescence and fluorescence microscopy

Cells were plated on cover slips, and the indicated treatments were then conducted. Cells were fixed with freshly prepared 4% paraformaldehyde at room temperature for 15 min following washed with phosphate-buffered saline (PBS). Then cells were permeabilized with PBS containing 0.1% Triton X-100 and 0.5% BSA at room temperature for 10 min. Subsequently, cells were incubated with the indicated primary antibodies at 4 °C overnight. After washing three times, cells were incubated with the secondary antibodies for 1 h at room temperature. The nuclei were stained by VECTASHIELD with DAPI (H1200) after washing three times. Images were acquired by fluorescence microscopy (Nikon). For mCherry-GFP-LC3B adenovirus (AD202001, Vigene Biosciences, Shandong, China) transfection cells, cells were fixed with freshly prepared 4% paraformaldehyde, and then washed three times with PBS. VECTASHIELD with DAPI (H1200) was added to the cells to visualize nuclei, and images were acquired by fluorescence microscopy (Nikon).

#### Chromatin immunoprecipitation (ChIP) assays

BeyoChIP™ ChIP Assay Kit (Protein A/G Magnetic Bead) (P2080S, Beyotime) was employed to conduct the ChIP assay, and the experiment followed the manufacturer's instructions. In brief, $4\times10^6$ cells were crosslinked with 1% formaldehyde for 10 min at 37 ℃, and then the reaction was stopped by glycine. Cells were collected, and cell nucleuses were prepared and treated with Micrococcal Nuclease (D7201S, Beyotime) to obtain 400–800 bp DNA fragments. Whereafter, chromatin immunoprecipitation was performed with the indicated primary antibody as well as Protein A/G Magnetic Beads, and then the crosslinked DNA was separated at 65℃ for 2 h and purified with DNA Clean-up Kit (CW2301S, CWBIO, China). ChIP samples were subjected to PCR and agarose gel electrophoresis to perform quantitative analysis. The sequences of primers for amplification were as follows:

| Gene | Primer | Nucleotides |
|---|---|---|
| PKM2 | Forward (5′ → 3′)<br>Reverse (5′ → 3′) | TGCAGGATTCCAGAC CCTACT<br>GGCCGTTTTCCTCTT AGGACC |

#### Xenograft of CRC cells in nude mice models

The Ethics Committee of Lanzhou University has approved the experiment. All the mice were purchased from Beijing HFK Bioscience Co., LTD. (Beijing, China) and maintained in the Jining Medicine University facility under specific-pathogen-free (SPF) conditions. The mice were divided into groups randomly. The indicated cells with or without the specific agents were injected into the abdominal subcutaneous tissues of mice with 0.1 mL ($1\times10^7$ cells/mL) to construct xenografts of CRC cells in nude mice.

Xenografts of CRC cells in nude mice were constructed firstly, and then the API-2 (1 mg/kg) as well as Shikonin (1 mg/kg) was intraperitoneally injected three times per 3 days, respectively. The tumors were gained after 20 days of inoculation. Simultaneously, the tumor volumes as well as weights were measured and recorded. Subsequently, the indicated molecules were examined by HE and IHC staining.

#### Statistical analysis

The data was shown as mean ± S.D. The two-sided Student' s t test was utilized to analyze the statistical significance between two groups' comparison, and the one-way ANOVA was used among multiple groups' comparisons. $P<0.05$ was regarded as statistical significance. Most of the data was gained from three independent experiments.

## Results

#### SULT2B1 as a high-risk factor is highly expressed in CRC

The transcriptional levels of SULT2B1 in pan-cancer were analyzed by bioinformatics, which showed SULT2B1 is highly expressed in numerous types of

tumors, such as BLCA, BRCA, ESCA, LUAD and so on (Figure S1A). When focused solely on CRC, likewise, the transcriptional level of SULT2B1 was highly expressed compared to normal tissue in both COAD and READ datasets from the TCGA (Figure S1B and C). Moreover, the expression levels of SULT2B1 were higher in stage IV patients than in the other three stages (Figure S2A), and those in CRC patients with distant metastasis (M1) were also significantly higher compared to patients with no distant metastasis (M0) ($p=0.0068$), indicating that the expression level of SULT2B1 was related to the terminal stages, M and N (Lymph Node) (Figure S2B and C). On the contrary, there was no correlation between SULT2B1 expression and age, gender or T (Topography) (Figure S2D). Additionally, the nomogram and calibration curve showed that three factors, including SULT2B1 expression, age and stage, had statistical significance in predicting the OS of CRC patients accurately (Figure S2E and F).

In a CRC tissue microarray (50 CRC specimens and 50 matched intestine specimens), the level of SULT2B1 in the cancer biopsies was significantly higher compared with the matched normal tissues (Fig. 1A, B). We then monitored its expression in 9 pairs of CRC and the adjacent normal tissues by immunoblotting assay, and the protein expression levels of SULT2B1 were higher in 8 tumor tissues of all tested cases (Fig. 1C). The Kaplan–Meier OS curve showed that high SULT2B1 expression portends a poor prognosis in CRC patients in the GEPIA database ($p=0.02$, $HR=1.7$) (Fig. 1D). Then, we detected the expression of SULT2B1 in several CRC cell lines and it is highly expressed in HT29, and lowly expressed in SW480 at both transcription and translation levels (Fig. 1E, F). Therefore, HT29 and SW480 cells were selected for the subsequent research.

#### SULT2B1 positively modulates proliferation, migration and invasion in CRC cells

Utilizing CRISPR-Cas9-gRNA targeted to SULT2B1 and Flag-SULT2B1 plasmids, we generated the SULT2B1 knockout HT29 cell line and the SULT2B1 overexpressed SW480 cell line, respectively (Fig. 2A). In MTS assay, we observed that knockout of SULT2B1 reduced cell viability, while its overexpression showed a promotion effect at both 24 h and 48 h time points (Fig. 2B). Meanwhile, its expression levels were associated with cell proliferation as monitored by the colony growth assay (Fig. 2C). Utilizing wound healing and trans-well assays, we found that its knockout cells exhibited a wider unhealed area and fewer invaded cells when compared with the KO-Ctrl group, while OE-SULT2B1 showed the opposite phenotypes (Fig. 2D, E). We then performed flow cytometry to detect the cell cycle, and the results showed that the percentage of S phase cells in the KO-SULT2B1 group was lower than that in the control group, while the OE-SULT2B1 group had the opposite trend (Fig. 2F). Similarly, the EDU staining assay displayed that the SULT2B1 level was positively associated with the percentage of EDU-positive cells, which replace thymine during the DNA replication process (Fig. 2G). Furthermore, we monitored the protein levels of several cyclin-dependent kinases and cell cycle inhibitors by immunoblotting assay. The results showed that KO-SULT2B1 reduced CDK2/4/6, and upregulated p21/p27 levels, while OE-SULT2B1 exhibited the opposite results (Fig. 2H, I). Moreover, we found that KO-SULT2B1 enhanced the cytotoxicity of Cisplatin (DDP), by monitoring the apoptotic cell death through both flow cytometry and immunoblotting assays (Figure S3). The abovementioned data indicated that SULT2B1 positively modulates cell proliferation/migration, and its knockout enhances chemo-sensitivity in CRC cells.

#### SULT2B1 accelerates CRC cells proliferation and migration by modulating AKT signaling pathway

We then performed GO and KEGG analyses, and the results showed that SULT2B1 engages in various biological processes related to the AKT/mTOR signaling pathway (Figure S4A–E). Furthermore, SULT2B1 possessed a positive correlation with AKT1 as well as AKT2 (Figure S4F and G). On the contrary, a negative correlation between SULT2B1 and AKT3 was obtained (Figure S4H). From CPTAC samples, the CRC tissues with mTOR signaling altered showed a significant higher SULT2B1 expressional level (Figure S4I).

In the CRC and the adjacent normal tissues, the p-mTOR, p-P70 and t-AKT levels were higher in the majority of CRC tissues (Fig. 3A). Meanwhile, KO-SULT2B1 reduced the protein levels of p-mTOR, p-P70 and p-AKT, while OE-SULT2B1 yielded the opposite results (Fig. 3B). In the OE-SULT2B1 SW480 cells, we performed the co-immunoprecipitation assay with Flag antibody, and the results indicated that there was an interaction between SULT2B1 and AKT (Fig. 3C). Moreover, SULT2B1 and AKT showed co-localization in the immunofluorescence assay, as observing the coexistence of red and green dots merging into yellow dots (Fig. 3D). Utilizing the GST pull-down assay, we further verified that these two proteins could interact with each other directly (Fig. 3E, F). Then we monitored whether AKT was involved in the cell fate determined by SULT2B1. SC79 [23], a specific agonist of AKT, was found to increase the levels of p-mTOR, p-p70 as well as p-AKT in both KO-Ctrl and KO-SULT2B1 cells (Fig. 3G). Moreover, SC79 partly rescued the cell viability loss and cell proliferation blockage aroused by SULT2B1 knockout (Fig. 3H, I). In the wound healing assay, SC79 treatment also decreased the wound area when compared

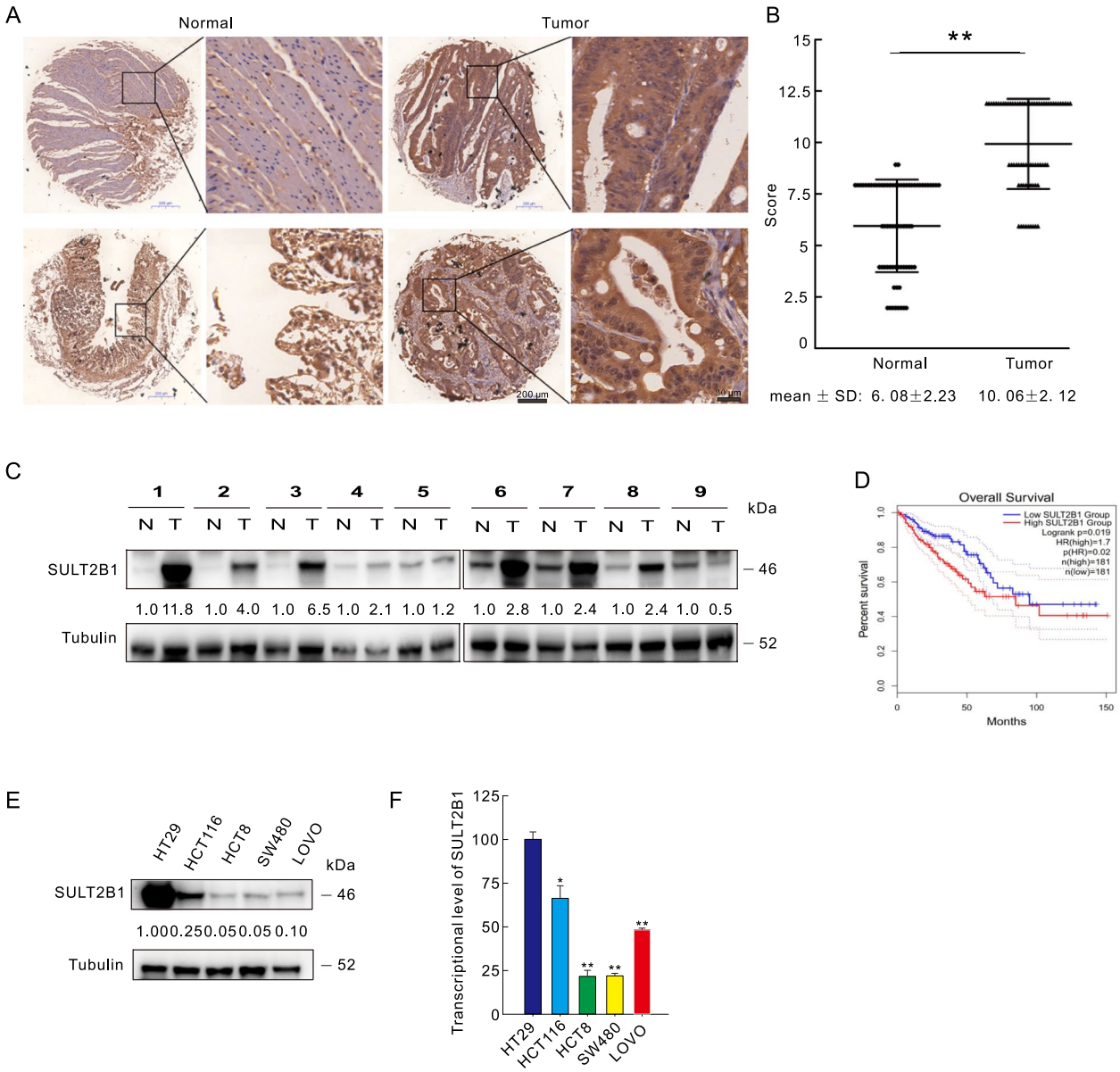


**Fig. 1** Expression and transcription levels of SULT2B1 in CRC tissues and cell lines. **A** and **B** Representative images and quantification analysis of SULT2B1 immunohistochemistry in a human CRC tissue microarray. Scale bars = 200 μm and 20 μm. **C** The expression levels of SULT2B1 in CRC surgical specimens and the matched adjacent intestinal tissues were detected by immunoblotting. **D** The Kaplan–Meier overall survival analysis between SULT2B1 expression and CRC in the GEPIA database. **E** Immunoblotting was used to determine the expression levels in CRC cell lines. **F** mRNA levels of SULT2B1 in CRC cell lines were monitored by RT-PCR. Data representing mean ± S.D. were shown in the graph. *P < 0.05 versus control; **P < 0.01 versus control

(See figure on next page.)

**Fig. 2** SULT2B1 promotes cell proliferation and migration in CRC cells. **A** KO-SULT2B1 HT29 cells and OE-SULT2B1 SW480 cells were constructed as described in methods, and efficacies were confirmed by immunoblotting. **B** Cell viability was detected by MTS assay. **C** Colony growth assay was conducted to monitor cell proliferation ability (scale bars = 1 cm). **D** Wound healing test was performed in the indicated cells, and pictures were taken at 0 h as well as 24 h time points (scale bars = 0.5 mm). **E** Transwell assay was carried out to monitor cell invasion (scale bars = 0.5 mm). **F** Indicated cells were collected and stained, and then flow cytometry was performed to analyze cell cycle. **G** EDU staining assay was conducted to detect cell proliferation (scale bars = 0.5 mm). **H** and **I** The lysates were prepared from indicated cells, and analyzed by immunoblotting with indicated antibodies. *P < 0.05 versus control; **P < 0.01 versus control

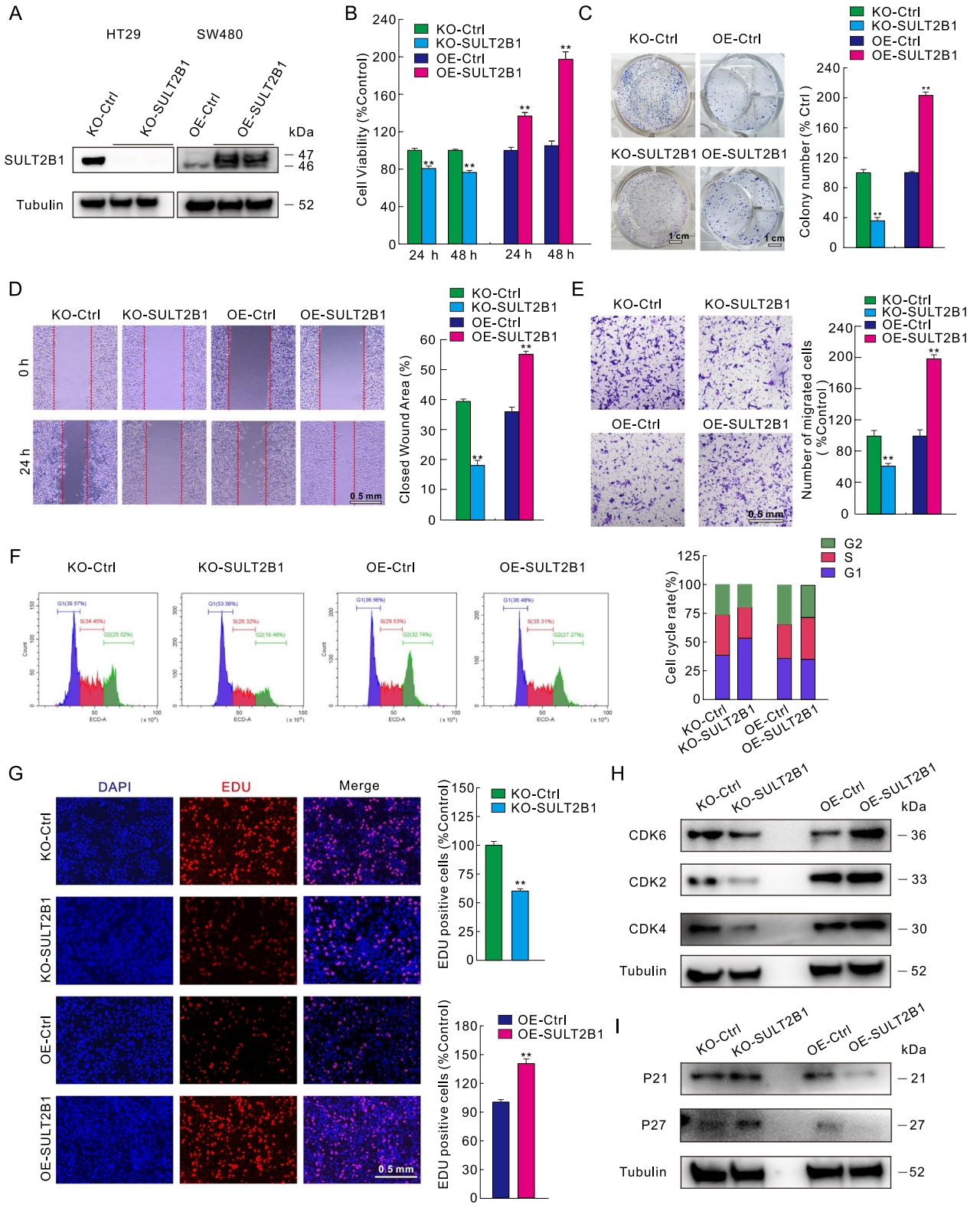


**Fig. 2** (See legend on previous page.)

to the control group, especially in the KO-SULT2B1 cells (Fig. 3J). In addition, the p21 and p27 protein levels decreased upon SC79 treatment (Fig. 3K). These results indicated that SULT2B1 could interact with and activate AKT, and its activation partly rescued cell proliferation/migration inhibited by SULT2B1 knockout. In the rescue experiment, transfection of Flag-SULT2B1 into KO-SULT2B1 cells obviously rescued the cell viability, cell proliferation and migration attenuated by SULT2B1 knockout (Figure S5A–D). Re-expression of SULT2B1 in the KO cells reduced the protein levels of both p21 and p27 (Figure S5E). Furthermore, overexpression of SULT2B1 in KO-SULT2B1 cells could reverse the decrease of p-mTOR, p-P70, as well as p-AKT (Figure S5F).

#### SULT2B1 promotes cell proliferation in vivo

To elucidate whether SULT2B1 can promote CRC cell proliferation in vivo, xenografts of CRC cells were constructed in nude mouse models. Knockout of SULT2B1 reduced the tumor volumes and weights, while OE-SULT2B1 increased tumor growth (Fig. 4A–D). Then the mice were euthanized, and the whole tumors were separated and pictured as shown in Fig. 4E, F. Furthermore, the HE and IHC staining also showed that knockout of SULT2B1 reduced the expression of ki-67 and p-/t-AKT, while its overexpression enhanced the ki-67 and p-/t-AKT levels (Fig. 4G–K). Then the whole proteins were extracted from the tumor tissues, and p21 as well as p27 were determined by immunoblotting. The results manifested that p21 and p27 were both higher in KO-SULT2B1 mouse tissues, while lower in OE-SULT2B1 mouse tissues (Fig. 4L).

#### Deprivation of AKT blunts the role of SULT2B1 in regulating cell proliferation

As a widely used inhibitor of AKT [24], API-2 obviously reduced the protein levels of p-mTOR, p-P70, and p-AKT in both OE-Ctrl and OE-SULT2B1 cells (Figure S6A). Meanwhile, API-2 remarkably attenuated the cell viability, proliferation and migration promoted by SULT2B1 overexpression (Figure S6B–D). Besides, API-2 increased the expression of P27 and P21 in both OE-Ctrl and OE-SULT2B1 cells (Figure S6E). To avoid the off-target effect of the antagonist, targeted siRNA was transfected into SW480 cells to decrease the expression of AKT1/2. Knockdown of AKT1/2 effectively blunted the protein levels of p-mTOR, p-P70 and p-AKT upregulated by SULT2B1 overexpression (Figure S6F). As expected, silencing of AKT1/2 attenuated cell viability and proliferation in both OE-Ctrl and OE-SULT2B1 cells (Figure S6G and H). Meanwhile, the levels of p21 and p27 were higher in the siAKT1/2 group than in the Mock control group (Figure S6I).

#### PKM2 combining with SULT2B1 contributes to cell proliferation and migration regulated by SULT2B1

The AKT signaling network affects multiple metabolic pathways, we then explored whether any other molecules functioned downstream of SULT2B1. Therefore, we performed immunoprecipitation with both Flag and SULT2B1 targeted antibodies in OE-SULT2B1 and OE-Ctrl cells, and subjected them to proteomic identification, respectively (Fig. 5A). Several shared proteins were identified, and we then focused on the glycolytic enzyme PKM2, and its interaction with SULT2B1 was verified by immunoprecipitation and immunofluorescence (Fig. 5B, C). By means of immunoblotting analysis, PKM2 was found to be lower in KO-SULT2B1 cells, while higher in OE-SULT2B1 cells when compared with control cells, respectively (Fig. 5D). Additionally, PKM2 was highly expressed in tumor tissue in the surgical specimens of CRC patients (Figure S7A). Then PKM2 overexpression cell lines were constructed, and the efficacy was confirmed (Figure S7B and C). Overexpression of PKM2 promoted cell proliferation and migration, and knockout of SULT2B1 failed to obviously reverse these processes (Fig. 5E–J). Consistently, knockout of SULT2B1 only enhanced the protein levels of p21 and p27 in OE-Ctrl cells, but not OE-PKM2 cells (Fig. 5K).

We also investigated the relationship between SULT2B1 and PKM2 with the help of Shikonin and

(See figure on next page.)

**Fig. 3** SULT2B1 accelerates CRC cell proliferation and migration by modulating the AKT signaling pathway. **A** The whole proteins were extracted from pairwise CRC and adjacent tissues, and then immunoblotting was conducted with the indicated antibodies. **B** Immunoblotting was used to monitor specific molecule expressions in KO-SULT2B1 HT29 and OE-SULT2B1 SW480 cell lines. **C** Co-immunoprecipitation was performed with Flag primary antibody in OE-SULT2B1 lysates. **D** Immunofluorescence co-localization was conducted with SULT2B1 and AKT primary antibody (Green dots: SULT2B1; Red dots: t-AKT; Arrow: Yellow dot represent co-localization). **E** and **F** GST pull-down assay was carried out, and the interaction between SULT2B1 and AKT was then monitored by gel stain and immunoblotting. **G** After treatment with SC79 (10 μM hereafter unless otherwise indicated) for 8 h, the lysates were prepared and subjected to immunoblotting with indicated antibodies. **H**–**J** MTS assay, colony growth assay (H: 1 μM) and wound healing assay were performed to detect the cell proliferation and migration abilities in cells with SC79 treatments (scale bars = 1 cm and 0.5 mm). **K** The P21 and P27 expressions were detected by immunoblotting in HT29 cells with the indicated treatments. *P < 0.05 versus control; **P < 0.01 versus control

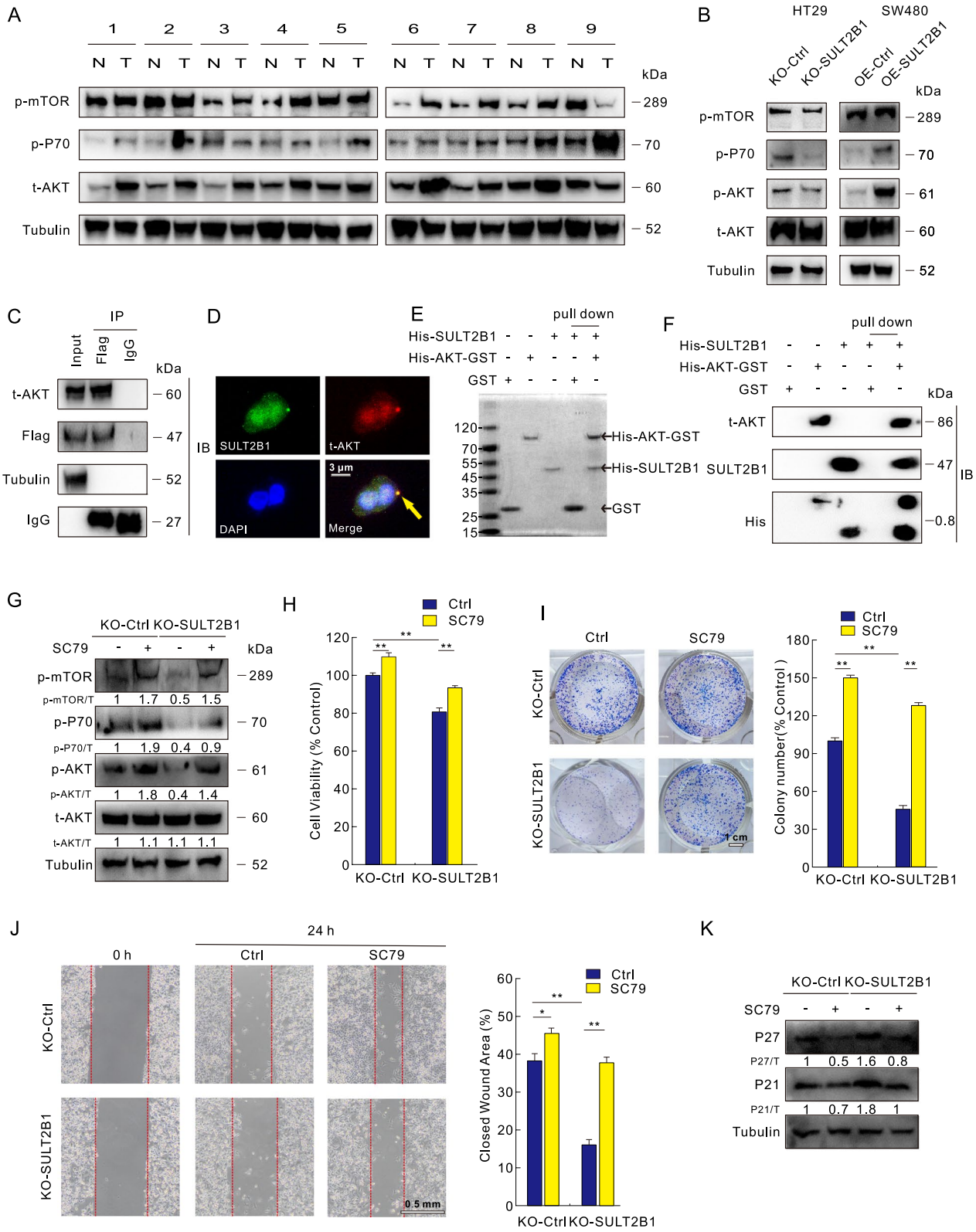


**Fig. 3** (See legend on previous page.)

Tepp46, which are considered as the small-molecule antagonist and agonist of PKM2, respectively [25, 26]. Inhibition of PKM2 by Shikonin obviously reduced cell proliferation and migration, and OE-SULT2B1 failed to play promoting roles upon Shikonin treatment in SW480 cells (Figure S7D–F). Knockout of SULT2B1 attenuated cell proliferation and migration in control cells, but not in the Tepp46-treated HT29 cells (Figure S7G and H). Furthermore, Shikonin increased, while Tepp46 decreased the levels of p21 and p27, respectively (Figure S7I and J). At the same time, modification of the expression of SULT2B1 failed to obviously alter the p21 and p27 levels upon both shikonin and Tepp46 treatment (Figure S7I and J). The abovementioned results implied that PKM2 functioned downstream of SULT2B1.

### SULT2B1 positively modulates the transcription of PKM2 by c-MYC and reduces the degradation of PKM2 by autophagy

It is known to all that c-MYC, a downstream transcription factor of the AKT/mTOR pathway, plays an indispensable and vital role in the transcription progression of cells [27]. Given this, immunoblotting was used to identify c-MYC expression in both Ctrl and KO-SULT2B1 HT29 cells. The findings demonstrated that c-MYC expression was reduced by SULT2B1 knockout, while SULT2B1 overexpression exhibited an opposite tendency (Fig. 6A). Furthermore, c-MYC was predicted as one of transcription factors that promoted the transcription of PKM2 by means of the JASPAR public database (Fig. 6B). Subsequently, a ChIP test using the c-MYC primary antibody was used to confirm that c-MYC bound to the particular promotor region of PKM2. The results showed that KO-SULT2B1 cells had less c-MYC associated to that area of PKM2 than KO-Ctrl cells did (Fig. 6C). The aforementioned information uncovered that SULT2B1 positively modulated the transcription of PKM2 through c-MYC.

Generally, proteins in eukaryotic cells were degraded by two main ways (the ubiquitin–proteasome pathway and the autophagy pathway) [28]. We found that the total ubiquitin increased after SULT2B1 knockout (Fig. 6D). However, not enough ubiquitin bonded to PKM2 was verified by immunoprecipitation analysis (Fig. 6E). Furthermore, the content of P62 as the substrate of autophagy decreased, whereas p-ULK, Becklin-1 and LC3 contents increased after SULT2B1 knockout (Fig. 6F). On the contrary, the transcription of P62 increased while that of LC3 decreased in RT-PCR analysis, which indicated that the protein content changes were not due to the transcription level (Fig. 6G). Furthermore, chloroquine (CQ) as a retardant of autophagy [29], reversed the decrease of P62 by SULT2B1 knockout, while boosted the LC3 content (Fig. 6H). Besides, the mCherry-GFP-LC3B assay was also performed to monitor autophagic flux, which was based on the different stability of mCherry and GFP fluorescent proteins upon pH alteration. Compared with KO-Ctrl cells, KO-SULT2B1 cells showed showed more autophagosome punctate (yellow) as well as autolysosome punctate (sole red) (Fig. 6I, J). The addition of CQ blunted, while whereas serum glucose free (SGF, a widely used autophagy inducer) enhanced the differences between KO-Ctrl and KO-SULT2B1 cells (Fig. 6I, J). Utilizing immunofluorescence, we observed that PKM2 could co-localize with p62 and LC3 (Fig. 6K). In addition, inhibition of autophagy by CQ increased the protein level of PKM2 in both KO-Ctrl and KO-SULT2B1 cells (Fig. 6L). Thus, PKM2 degradation did not depend on the ubiquitin–proteasome pathway but on the autophagy pathway.

### Both AKT and PKM2 inhibitors repress the role of SULT2B1 in regulating cell proliferation in vitro and in vivo

As SULT2B1 regulated cell fate by modulating AKT and PKM2, we then explored the relationship between AKT and PKM2. In both KO-Ctrl and KO-SULT2B1 cells, the AKT agonist SC79 was found to increase the protein level of PKM2 (Figure S8A). On the contrary, inhibition of AKT by API-2 reduced PKM2 expression in both OE-Ctrl and OE-SULT2B1 cells (Figure S8A). In the API-2-treated cells, overexpression of PKM2 remarkably promoted cell proliferation and migration (Figure S8B–E). However, API-2 still inhibited the cell activity in OE-PKM2 cells, which may be due to the fact that AKT functions through other effector molecules bypass PKM2 (Figure S8B–E). Moreover, Shikonin reduced

(See figure on next page.)

**Fig. 4** SULT2B1 positively promotes cell proliferation in *vivo*. **A** and **C** Xenografts of CRC cells in nude mice were constructed, and the tumor volumes were calculated and recorded at the indicated time points (The time of tumor excision from euthanized mice, A: 25 day; C: 20 day). The data were analyzed and visualized by the Prism GraphPad software. **B** and **D** Tumor weights were recorded and shown. **E** and **F** The tumors were photographed and shown. **G** HE staining was performed to analyze cell proliferation in specific tumor tissues (scale bars = 150 μm). **H**–**K** IHC staining was conducted in indicated tumor tissues with SULT2B1, p-AKT, t-AKT and Ki67 primary antibodies and quantification analysis was performed (scale bars = 50 μm and 6 μm). **L** Immunoblotting was carried out to detect the expressions of indicated molecules in xenografts tumors. *P < 0.05 versus control; **P < 0.01 versus control

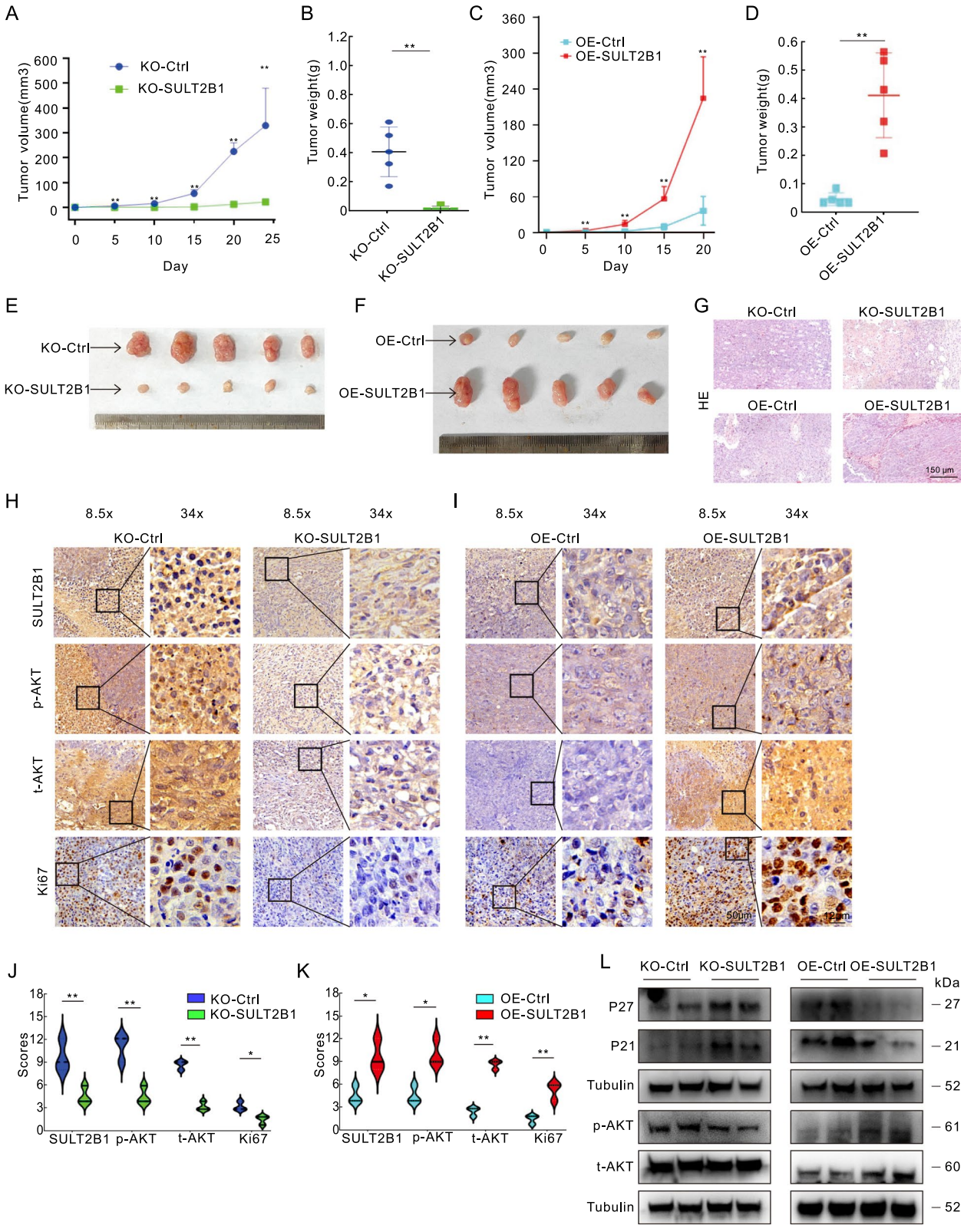


**Fig. 4** (See legend on previous page.)

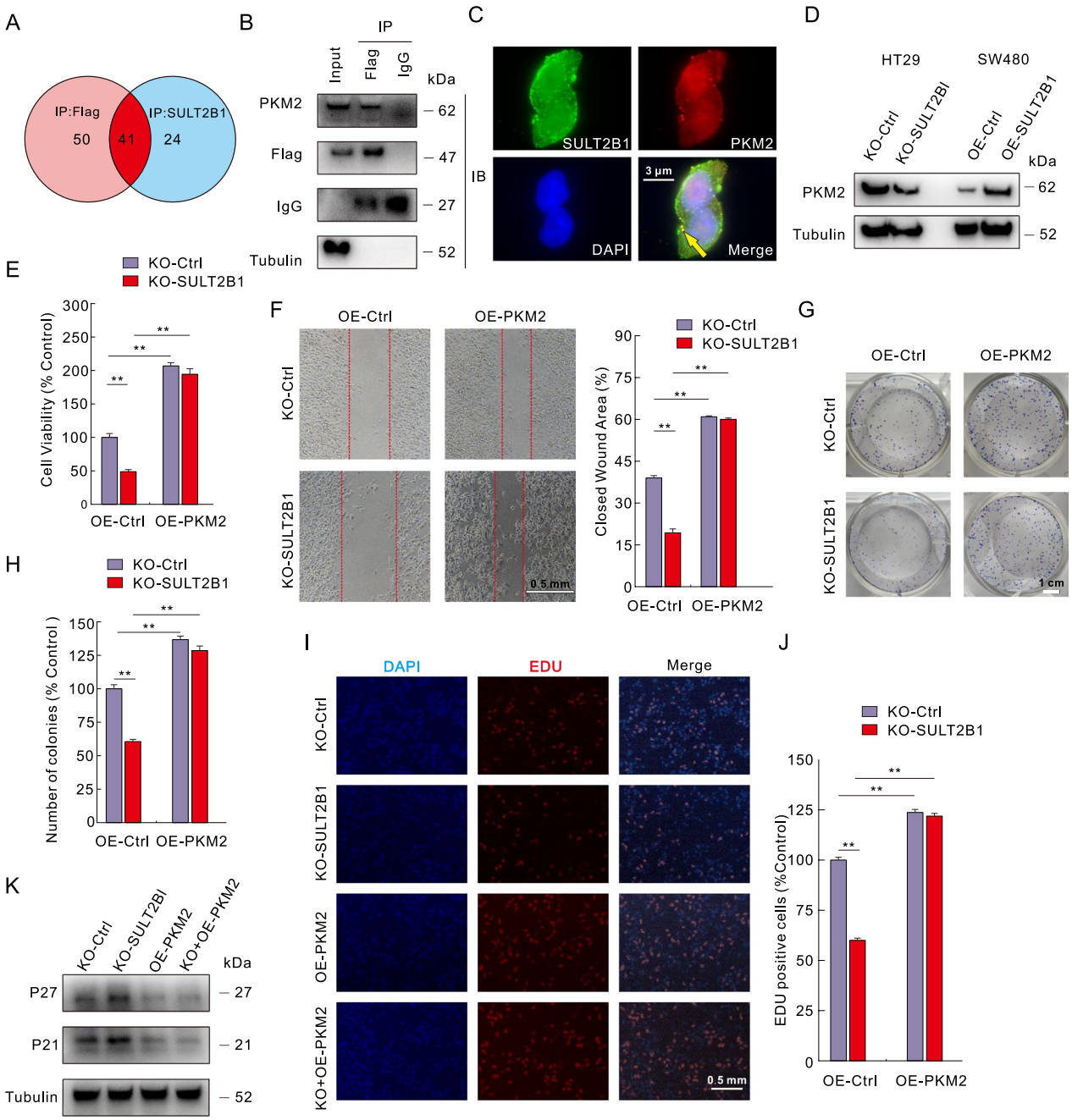


**Fig. 5** PKM2 combing with SULT2B1 contributes to the cell proliferation and migration regulated by SULT2B1. **A** Immunoprecipitation was performed with Flag and SULT2B1 targeted antibodies in OE-SULT2B1 and OE-Ctrl cells, respectively, and then the lysates were subjected to proteomic identification. **B** Co-immunoprecipitation was performed with Flag primary antibody in OE-SULT2B1 lysates. **C** Immunofluorescence co-localization was conducted with SULT2B1 and PKM2 primary antibody in OE-SULT2B1 cells. **D** The PKM2 expression was monitored in the indicated cells by immunoblotting. **E**–**J** Cell proliferation and migration abilities in the indicated cells were analyzed by MTS assay, wound healing assay (scale bars = 0.5 mm), colony growth assay (scale bars = 1 cm) and EDU staining assay (scale bars = 0.5 mm). The data were visualized by histogram graphs. **K** The P21 and P27 expressions were determined by immunoblotting in the indicated cells. *P < 0.05 versus control; **P < 0.01 versus control

the cell activity with or without SC79 treatment (Figure S8F–I). Distinct from API-2, the inexplicable results were that the addition of SC79 failed to rescue the cell activity upon Shikonin treatment (Figure S8F–I), which probably resulted from the SULT2B1 knockout, but we cannot be certain yet. Nevertheless, it was convinced to conclude that SULT2B1 modulate PKM2 by affecting the AKT signaling.

To verify the results of in vitro experiments, the xenograft models in nude mice with OE-Ctrl and OE-SULT2B1 cells were constructed, and then treated with API-2 and Shikonin, respectively. Both API-2 and Shikonin diminished tumor volumes and weights (Fig. 7A–C). Then the mice were euthanized, and the whole tumors were separated and pictured as shown in Fig. 7D. Furthermore, both API-2 and Shikonin reduced the score of ki-67 in both OE-Ctrl and OE-SULT2B1 groups (Fig. 7E–G). In addition, we observed that both API-2 and Shikonin reversed the reduction of p21 and p27 by SULT2B1 overexpression (Fig. 7H). These abovementioned data demonstrated that SULT2B1 regulated cell proliferation by AKT and PKM2 signals in *vivo*.

### SULT2B1 positively regulates glycolysis via the AKT/PKM2 axis in CRC cells

As PKM2 was a rate-limiting enzyme in the glycolytic pathway, we then verified whether glycolysis was involved in SULT2B1-regulated cell proliferation and migration [30]. Lactic acid is the product of glycolysis, and can be used to reflect the level of glycolysis [31]. Overexpression of SULT2B1 increased the lactate content, while both API-2 and Shikonin obviously blunted its promotion effect (Fig. 8A, B). On the contrary, SC79 or OE-PKM2 reversed the reduction of lactate aroused by SULT2B1 knockout (Fig. 8C, D). In order to block the glycolysis process, we treated the cells with both glucose-free (GF) medium and 2DG, which is an analogue of glucose without the ability to participate in the subsequent glycolytic pathway [32]. 2DG and GF treatment could reduce cell proliferation and migration, and overexpression of SULT2B1 failed to significantly reverse these processes (Fig. 8E–H). Meanwhile, both 2DG and GF increased the level of P21 and P27 in both OE-Ctrl and OE-SULT2B1 cells (Fig. 8I). Therefore, SULT2B1 regulated glycolysis to promote cell proliferation and migration via the AKT/PKM2 axis.

## Discussion

Generally, SULT2B1 functions as an oncogene, which is highly expressed in cancer cells and promotes carcinogenesis in several kinds of cancers, including endometrial cancer, breast cancer, liver cancer and CRC [33]. However, Hong et al. implied that SULT2B1 knockout increased gastric tumor incidence by suppressing PI3K/AKT signaling and epithelial cell epithelization in mice [34]. Meanwhile, it has also been reported to rarely express in esophageal squamous cell carcinoma as well as prostate cancer, and its overexpression reduces cell proliferation in vitro and in vivo [35]. Therefore, the correlation between SULT2B1 expression and carcinogenesis is not completely consistent across different types of cancers. Here, we verified that SULT2B1 was highly expressed in the cancer biopsies of CRC, by means of bioinformatics analysis from the TCGA database, IHC staining of a CRC tissue microarray, as well as immunoblotting assay with 9 pairs of clinical samples (CRC and the adjacent normal tissues). Moreover, overexpression of SULT2B1 increased both cell proliferation and migration in vitro, and promoted tumor growth in the nude mice xenograft model. On the contrary, its knockout presented the opposite phenotypes. CDK2/4/6 are important

(See figure on next page.)

**Fig. 6** SULT2B1 regulates the transcription of PKM2 by c-MYC and promotes the degradation of PKM2 by autophagy. **A** The expression of c-MYC was monitored in the indicated cells by immunoblotting. **B** The JASPAR database was used to predict the binding sequences of c-MYC in the promoter of PKM2. **C** The ChIP assay was performed, and the DNA bound to c-MYC was subjected to PCR using the specific primer, followed by agarose gel electrophoresis analysis. **D** Total ubiquitin was detected in both KO-Ctrl and KO-SULT2B1 HT29 cells by immunoblotting. **E** The co-immunoprecipitation was conducted with the primary antibody of PKM2, and the immunoprecipitate was subjected to SDS-PAGE electrophoresis analysis. **F** and **G** Immunoblotting and RT-PCR were used to identify the particular molecules involved in autophagy. **H** Using immunoblotting, the P62 and LC3 contents in KO-Ctrl and KO-SULT2B1 cells treated with or without chloroquine (CQ) were examined. **I** and **J** Indicated cells were transfected with the mCherry-GFP-LC3 adenovirus, and then exposed to indicate treatment for 2 h. The pictures were obtained by fluorescence microscope. **K** Immunofluorescence was performed with indicated antibodies. (**L**) The content of PKM2 in the indicated cells, either with or without CQ treatment, was determined by immunoblotting

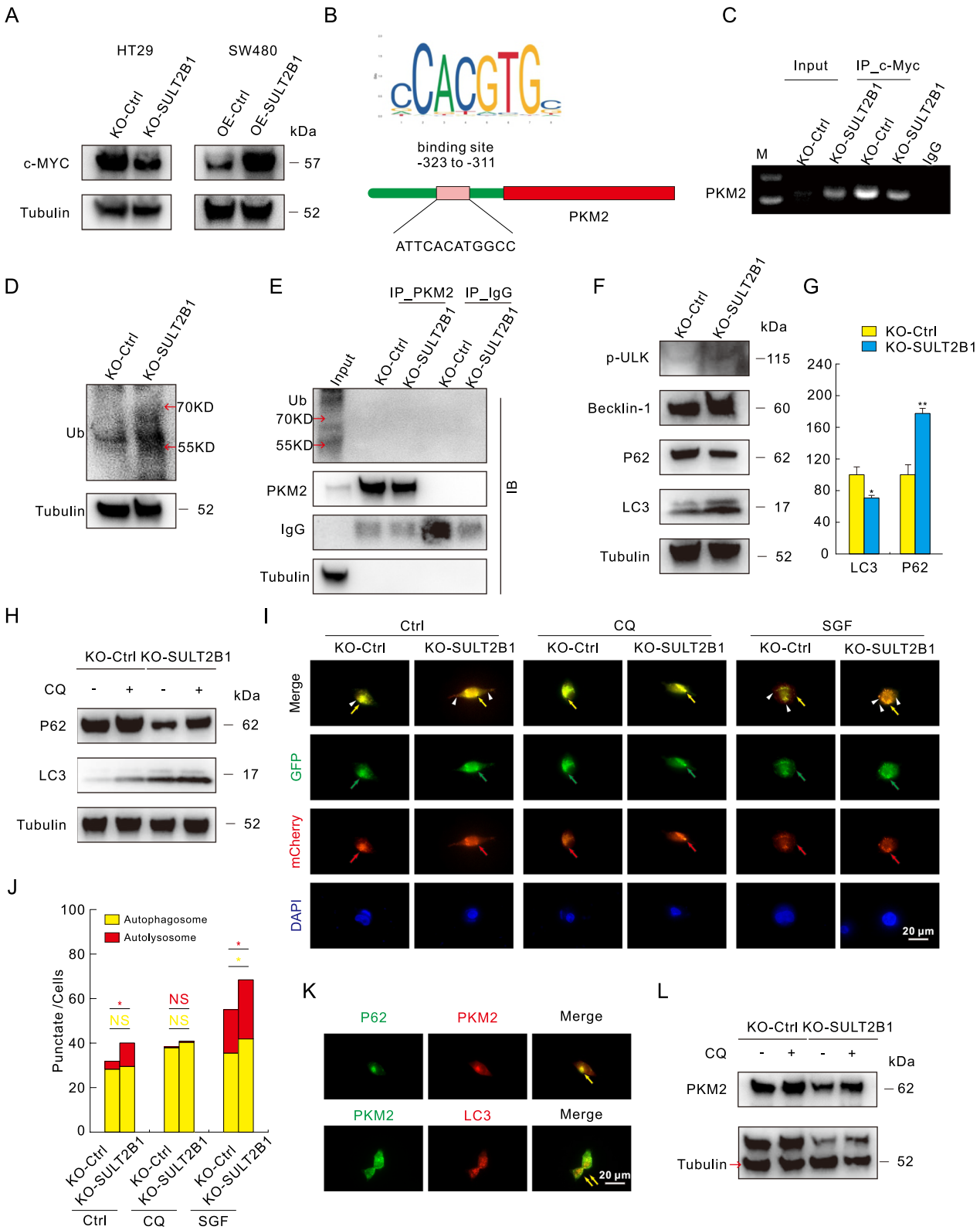


**Fig. 6** (See legend on previous page.)

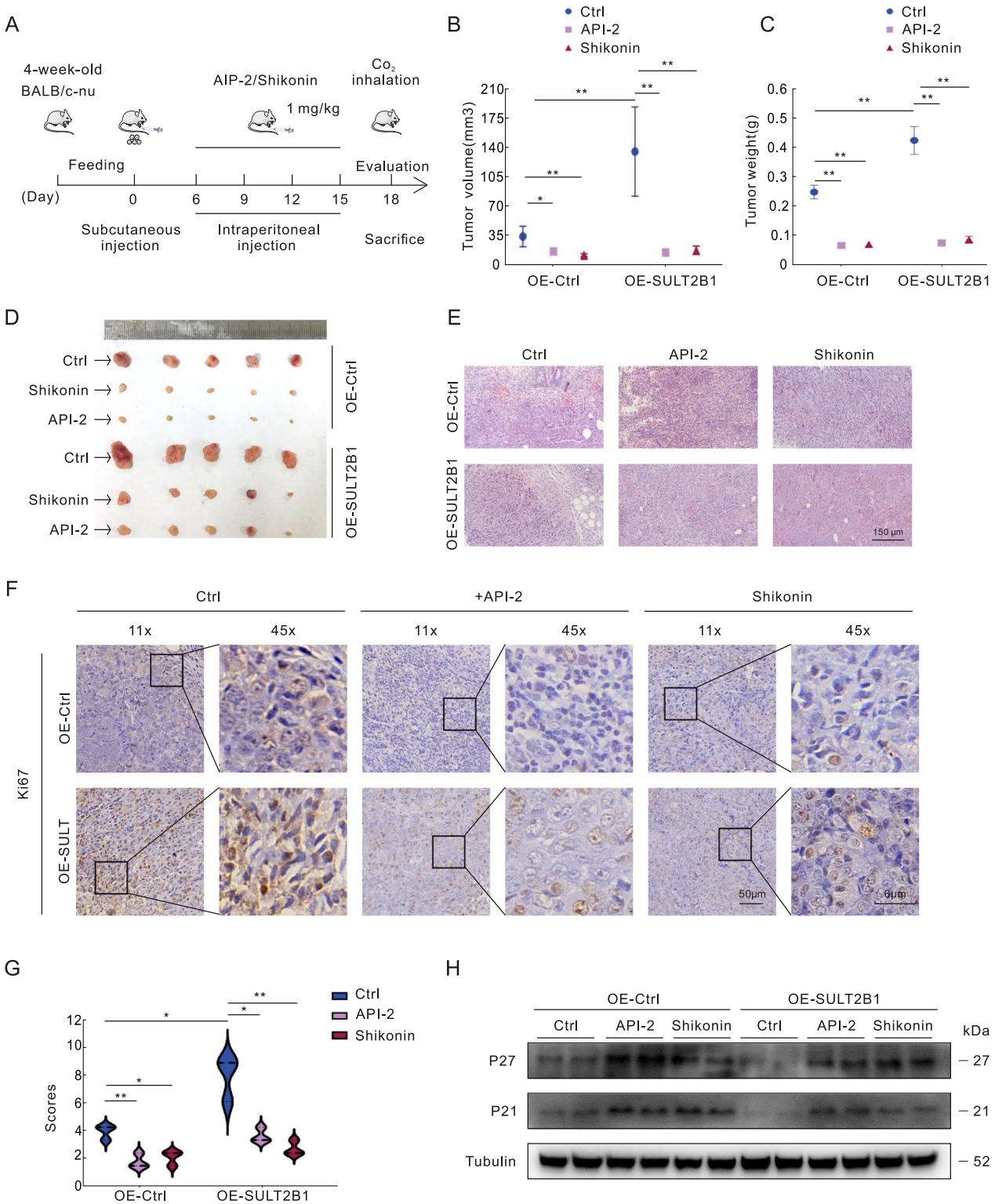


**Fig. 7** Both AKT and PKM2 inhibitors repress the role of SULT2B1 in regulating cell proliferation in *vivo*. **A** The schematic diagram of the animal experiment. **B**–**D** Xenograft mouse models in nude mice with OE-Ctrl and OE-SULT2B1 cells were constructed, and then treated with API-2 as well as Shikonin. The volume as well as weight of tumors were measured and visualized, and the photos of tumors in xenograft models were shown. **E**–**G** HE and IHC staining were conducted to analyze the cell proliferation in *vivo* as described above (scale bars = 50 μm and 6 μm). **H** The tumor tissues were grinded and lysed, and then the lysates were subjected to immunoblotting with indicated antibodies. *P < 0.05 versus control; **P < 0.01 versus control

component of the cell cycle machinery, and regulating cell proliferation process. Their activities were negatively modulated by the cell cycle inhibitors P21 and P27, which were generally considered to be the tumor suppressors [36]. In the present study, we observed that SULT2B1 positively regulated CDK2/4/6 levels, while negatively influencing the P21/P27 protein levels, indicating that it positively affected the cell cycle in CRC cells.

The AKT/mTOR signaling plays critical roles in regulating diverse cellular functions including metabolism, proliferation, and migration [37]. Although some reports showed a negative association with carcinogenesis [38], the AKT/mTOR signaling is generally dysregulated in cancer cells and considered to be [39]. All three isoforms of AKT have been reported to promote cell survival and proliferation in different cancer cells [40]. However, we observed that the level of SULT2B1 was positively correlated with AKT1 and AKT2, but not AKT3. Therefore, we focused on the former two isoforms of AKT in the current study. Inhibition of AKT by both its inhibitor and AKT1/2-targeted siRNA not only reduced the AKT/mTOR signaling activity, but also reversed cell proliferation/migration all of which were promoted by SULT2B1 overexpression. On the contrary, the agonist of AKT reversed the inhibitory effects of KO-SULT2B1 on cell fate determination. Utilizing the GST pull-down and Co-IP experiments, we confirmed that SULT2B1 could directly interact with at least AKT2. These results indicated that SULT2B1 functioned upstream of AKT/mTOR signaling by binding to and modifying the AKT activity. Due to our failure to distinguish between the roles of AKT1 and AKT2 here, we will investigate the functional AKT isoform and its binding domain with SULT2B1 in future studies.

Cancer cells are prone to a high rate of aerobic glycolysis even in normoxic conditions, a phenomenon known as the Warburg effect [41]. As one of the three rate-limiting enzymes in the glycolysis process, PKM2 has also been reported to participate in regulating metabolism, cell proliferation and carcinogenesis [20]. In the present study, PKM2 was screened out in the mass spectrometry identification of SULT2B1 immunoprecipitate, indicating that there was an intrinsic correlation between them. ChIP and mCherry-GFP-LC3 assay made clear that SULT2B1 positively regulated the transcription of PKM2 by c-MYC and attenuated the degradation of PKM2 by autophagy. Given previous reports of c-MYC positively regulating SULT2B1 expression [14], there may be a mutual regulation phenomenon between them that warrants further elucidation of the specific mechanism. Furthermore, we found a positive association between SULT2B1 and PKM2 expression, and the modification activity of PKM2 obviously altered the effect of SULT2B1 on cell proliferation and migration. For instance, overexpressing PKM2 promotes/rescues cellular viability and proliferation in KO-Ctrl/KO-SULTB21 cells, while knocking out SULT2B1 only exerts an inhibitory effect in OE-Ctrl cells, but not in OE-PKM2 cells. Both observations suggest that PKM2 exerts a more dominant influence than SULT2B1 on downstream effects, thereby functioning as the primary effector. Thus, PKM2 may function downstream of SULT2B1 in certain conditions. Although inconsistently reported, there are close connections between PKM2 and AKT, as PKM2 could function upstream, downstream, or in parallel with AKT in regulating different physiological and pathological processes [21, 22, 42, 43]. This may be due to the enormous complexity of signal transduction networks and the diversity of cell states. SC79 increased, while API-2 reduced the protein level of PKM2, and SC79 failed to rescue the cell viability loss induced by PKM2 inhibitor in KO-SULT2B1 cells, indicating that PKM2 functioned downstream of AKT in the cell fate regulated by SULT2B1 in CRC cells. Although the toxicity of API-2 has decreased when compared to OE-Ctrl cells, it can't be denied that API-2 still reduced cell viability, proliferation and migration in OE-PKM2 cells. This result may be due to the other signaling regulated by AKT, which requires further investigation.

In conclusion, the presented data clearly demonstrated that SULT2B1 promoted cell proliferation and migration in CRC cells. SULT2B1 not only influenced the protein levels of AKT and PKM2, but also interacted with both of them. With the help of small molecular agonist/antagonist and genetic modification, further exploration indicated that SULT2B1 regulates cell fate in an AKT/PKM2 axis-dependent manner. These results revealed an intimate relationship among SULT2B1, AKT signaling and glycolytic pathways, and provided a theoretical basis for SULT2B1 as a potential therapeutic target for CRC (Fig. 8J).

(See figure on next page.)

**Fig. 8** SULT2B1 positively regulates glycolysis via the AKT/PKM2 axis in CRC cells. **A**–**D** The supernatant of specific cells with indicated treatments for 8 h was collected, and the lactate content was monitored by the L-Lactic Acid Assay Kit. **E**–**H** EDU staining assay, colony growth assay, and wound healing test were performed to detect cell proliferation as well as migration with 2DG (**F**: 1 mM; **E**, **G**: 10 mM) and GF treatments (scale bars = 0.5 mm and 1 cm). **I** Immunoblotting was carried out to determine the expressions of P21 and P27 after indicated treatment for 8 h. **J** The schematic model of SULT2B1 modulates the CRC cell progression via the AKT/PKM2 axis. *P < 0.05 versus control; **P < 0.01 versus control

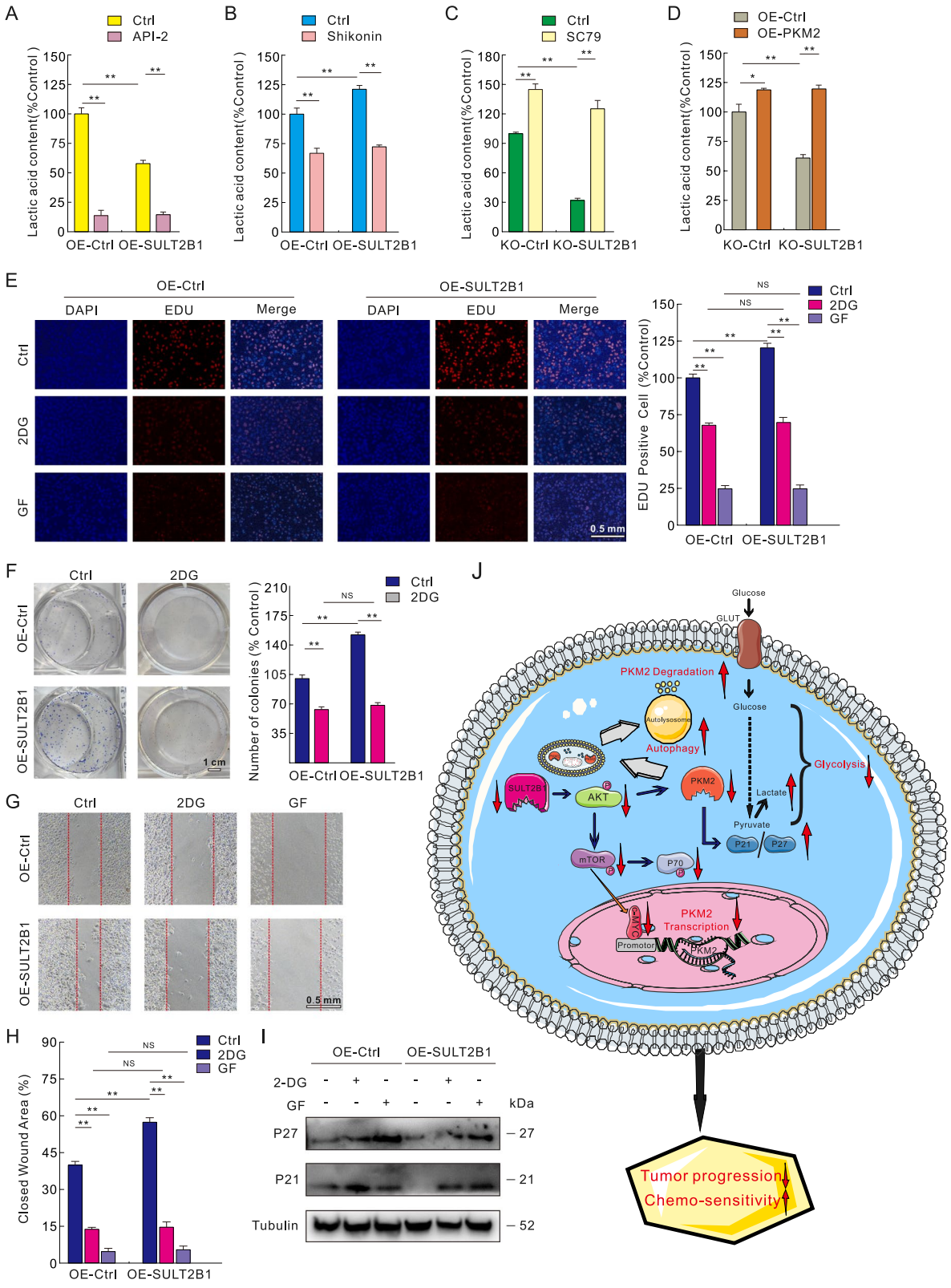


**Fig. 8** (See legend on previous page.)

## Supplementary Information

The online version contains supplementary material available at https://doi.org/10.1186/s12967-024-05910-4.

Supplementary material 1: Figure S1. The transcription level of SULT2B1 in cancer.Transcriptional levels of SULT2B1 in pan cancer were analyzed in the TIMER database.The unpaired and pairwise differences of SULT2B1 at the transcription level in 42 normal and 491 tumor tissues in the combined the TCGA-COAD and TCGA-READ datasets. * P < 0.05 versus control; **P < 0.01 versus control. Figure S2. Analysis of clinical correlation of SULT2B1 in combining the TCGA-COAD and TCGA-READ datasets.Analysis of correlation between the SULT2B1 expression and clinical characteristics in combined the TCGA-COAD and TCGA-READ datasets.Nomograph for OS prediction and calibration curve for the judgment of accuracy. *P < 0.05 versus control; **P < 0.01 versus control. Figure S3. SULT2B1 knockout boosts chemo-sensitivity in CRC cells. Flow cytometry and immunoblotting were conducted to detect the apoptotic cell death following treatments with the 10 ug/L final concentration of cisplatinfor 24 h in KO-Ctrl and KO-SULT2B1 HT29 cells. Figure S4. The bioinformatics analysis shows that SULT2B1 regulates tumor progression via the AKT signaling pathway.The TCGA-COAD and TCGA-READ data were downloaded from the TCGA database. GO and KEGG analyses of SULT2B1 were conducted by R 4.2.2.Analyses of the correlation between SULT2B1 expression and AKT1, AKT2, as well as AKT3 were performed with the data downloaded from the TCGA database by R 4.2.2.Analysis of correlation at the expression level between SULT2B1 expression and AKT/mTOR pathway-altered in CPTAC samples of the UALCAN database. *P < 0.05 versus control; **P < 0.01 versus control. Figure S5. SULT2B1 overexpression rescues the diminishment of CRC cell proliferation and migration aroused by SULT2B1 knockout.After transfecting OE-SULT2B1 plasmids into KO-SULT2B1 HT29 cells, the efficacy was confirmed by immunoblotting. KO+OE: Re-expression of SULT2B1 in KO-SULT2B1 HT29 cells.The cell migration and proliferation activities were analyzed by wound healing test, MTS assay and colony growth assay.Immunoblotting was performed with the indicated antibodies in specific cells. *P < 0.05 versus control; **P < 0.01 versus control. Figure S6. Inhibition of AKT blunts the role of SULT2B1 in positively regulating cell proliferation.The whole proteins were extracted from cells with API-2 treatments for 8 h, and immunoblotting was carried out to detect specified molecule expressions with the indicated primary antibodies.MTS assay, colony growth assayand wound healing testwere performed to monitor the cell proliferation and migration following the indicated treatments.Immunoblotting was performed to determine the expression levels of P21 and P27.After successfully interfering with the expression of AKT 1/2, the cells were collected and lysed. Then the lysates were subjected to immunoblotting with the indicated antibodies. MTS assay and colony growth assay were conducted to analyze the cell proliferation ability of the indicated cells.Immunoblotting was utilized to determine the P21 and P27 expressions in the indicated cells. *P < 0.05 versus control; **P < 0.01 versus control. Figure S7. Both AKT and PKM2 inhibitors suppresses the role of SULT2B1 in regulating CRC cell proliferation in *vivo*.Immunoblotting analysis was utilized to detect PKM2 expression levels in normal and tumor surgical tissues of CRC patients. The efficacies of PKM2 overexpression in SW480 and HT29 cells were verified by immunoblotting, and fluorescent pictures were taken.MTS assay, colony growth assayand wound healing testwere performed to analyze the indicated cell proliferation and migration with Shikonin treatments. Cell proliferation and migration were monitored by colony growth assay as well as wound healing testin KO-Ctrl and KO-SULT2B1 HT29 cells with the 10 μM Tepp46.P21 and P27 were determined by immunoblotting in the indicated cells with specific treatments for 8 h. *P < 0.05 versus control; **P < 0.01 versus control. NS: not significant. Figure S8. AKT functions upstream of PKM2.The PKM2 expression levels were detected by immunoblotting in indicated cells upon SC79 or API-2treatment for 8 h.The OE-Ctrl and OE-PKM2 SW480 cells were constructed by lentivirus infection. MTS assay, colony growth assay and wound healing test were conducted to analyze the cell proliferation as well as migration in the indicated cells with API-2 treatments.The P21 and P27 expressions were monitored in the indicated cells by immunoblotting.The cell proliferation and migration abilities were detected by MTS assay, colony growth assay and wound healing test in KO-Ctrl and KO-SULT2B1 HT29 cells with the indicated treatments.Immunoblotting was carried out to determine the P21 and P27 expressions in the indicated cells with specific treatments for 8 h. *P < 0.05 versus control; **P < 0.01 versus control.

Supplementary material 2: Table S1. The detailed information of antibodies. Table S2. Patients' information. The table listed the patients' information of the tumor samples used in the current study, who were underwent surgical treatment at the Second Hospital of Lanzhou University from 2021 to 2022. It contains ID number, Sex, Age, pathology information and so on. Table S3. The List of Protein Identified by Proteomics from Figure 5A.

**Acknowledgements**
We thank Dr. Shanshan Wang for the supply of the Ki67 primary antibody.

**Author contributions**
Jianxing Ma: Data curation, Investigation, Software, Writing – original draft; Fengyao Sun: Investigation, Methodology; Wen Li: Investigation; Ruihang Du: Investigation; Mingchan Liu: Investigation; Qiuya Wei: Investigation, Software; Boxiong Kang: Investigation, Software; Siyuan Yan: Conceptualization, Data curation, Funding acquisition, Supervision, Chen Wang: Supervision, Writing – review & editing.

**Funding**
This work was supported by grants from the National Natural Science Foundation of China (31801169), the Shandong Provincial Natural Science Foundation (ZR2023MH329), the Project of Shandong Province Higher Educational Youth Innovation Science and Technology Program (2023KJ263), and the Scientific and Technological Innovation Program of Lanzhou University Second Hospital (CY2023-QN-B01).

**Availability of data and materials**
All data generated or analyzed during this study are included in this published article and its supplementary information files.

## Declarations

**Ethics approval and consent to participate**
All animal experiments were conducted in accordance with the guidelines of the Animals Administrative Committee of Lanzhou University.

**Consent for publication**
Not applicable.

**Competing interests**
The authors state that there are no conflicts of interest to declare.

Received: 14 September 2024 Accepted: 21 November 2024
Published online: 02 December 2024

**References**

1. Sung H, Ferlay J, Siegel RL, Laversanne M, Soerjomataram I, Jemal A, Bray F. Global Cancer Statistics 2020: GLOBOCAN estimates of incidence and mortality worldwide for 36 cancers in 185 countries. CA Cancer J Clin. 2021;71:209–49.
2. Shinji S, Yamada T, Matsuda A, Sonoda H, Ohta R, Iwai T, Takeda K, Yonaga K, Masuda Y, Yoshida H. Recent advances in the treatment of colorectal cancer: a review. J Nippon Med Sch. 2022;89:246–54.
3. Sadanandam A, Lyssiotis CA, Homicsko K, Collisson EA, Gibb WJ, Wullschleger S, Ostos LC, Lannon WA, Grotzinger C, Del Rio M, Lhermitte B, Olshen AB, Wiedenmann B, Cantley LC, Gray JW, Hanahan D. A colorectal cancer classification system that associates cellular phenotype and responses to therapy. Nat Med. 2013;19:619–25.
4. Falany CN, Rohn-Glowacki KJ. SULT2B1: unique properties and characteristics of a hydroxysteroid sulfotransferase family. Drug Metab Rev. 2013;45:388–400.

5. Heinz L, Kim GJ, Marrakchi S, Christiansen J, Turki H, Rauschendorf MA, Lathrop M, Hausser I, Zimmer AD, Fischer J. Mutations in SULT2B1 cause autosomal-recessive congenital ichthyosis in humans. Am J Hum Genet. 2017;100:926–39.
6. Bensinger SJ, Bradley MN, Joseph SB, Zelcer N, Janssen EM, Hausner MA, Shih R, Parks JS, Edwards PA, Jamieson BD, Tontonoz P. LXR signaling couples sterol metabolism to proliferation in the acquired immune response. Cell. 2008;134:97–111.
7. Xu D, Ma R, Ju Y, Song X, Niu B, Hong W, Wang R, Yang Q, Zhao Z, Zhang Y, Zheng Y, Bai Q, Lv M, Sun N, Li X. Cholesterol sulfate alleviates ulcerative colitis by promoting cholesterol biosynthesis in colonic epithelial cells. Nat Commun. 2022;13:4428.
8. Morino K, Kunimura K, Sugiura Y, Izumi Y, Matsubara K, Akiyoshi S, Maeda R, Hirotani K, Sakata D, Mizuno S, Takahashi S, Bamba T, Uruno T, Fukui Y. Cholesterol sulfate limits neutrophil recruitment and gut inflammation during mucosal injury. Front Immunol. 2023;14:1131146.
9. Wang Y, Jin H, Wang Y, Yao Y, Yang C, Meng J, Tan X, Nie Y, Xue L, Xu B, Zhao H, Wang F. Sult2b1 deficiency exacerbates ischemic stroke by promoting pro-inflammatory macrophage polarization in mice. Theranostics. 2021;11:10074–90.
10. Chen W, Zhou H, Ye L, Zhan B. Overexpression of SULT2B1b promotes angiogenesis in human gastric Cancer. Cell Physiol Biochem. 2016;38:1040–54.
11. Yang X, Xu Y, Guo F, Ning Y, Zhi X, Yin L, Li X. Hydroxysteroid sulfotransferase SULT2B1b promotes hepatocellular carcinoma cells proliferation in vitro and in vivo. PLoS ONE. 2013;8:e60853.
12. Hu L, Yang GZ, Zhang Y, Feng D, Zhai YX, Gong H, Qi CY, Fu H, Ye MM, Cai QP, Gao CF. Overexpression of SULT2B1b is an independent prognostic indicator and promotes cell growth and invasion in colorectal carcinoma. Lab Invest. 2015;95:1005–18.
13. Huang J, Zhou M, Zhang H, Fang Y, Chen G, Wen J, Liu L. Characterization of the mechanism of Scutellaria baicalensis on reversing radio-resistance in colorectal cancer. Transl Oncol. 2022;24:101488.
14. Zhao T, Li Y, Shen K, Wang Q, Zhang J. Knockdown of OLR1 weakens glycolytic metabolism to repress colon cancer cell proliferation and chemoresistance by downregulating SULT2B1 via c-MYC. Cell Death Dis. 2021;13:4.
15. Revathidevi S, Munirajan AK. Akt in cancer: mediator and more. Semin Cancer Biol. 2019;59:80–91.
16. Tewari D, Patni P, Bishayee A, Sah AN, Bishayee A. Natural products targeting the PI3K-Akt-mTOR signaling pathway in cancer: a novel therapeutic strategy. Semin Cancer Biol. 2022;80:1–17.
17. Panwar V, Singh A, Bhatt M, Tonk RK, Azizov S, Raza AS, Sengupta S, Kumar D, Garg M. Multifaceted role of mTOR (mammalian target of rapamycin) signaling pathway in human health and disease. Signal Transduct Target Ther. 2023;8:375.
18. Chung S, Yao J, Suyama K, Bajaj S, Qian X, Loudig OD, Eugenin EA, Phillips GR, Hazan RB. N-cadherin regulates mammary tumor cell migration through Akt3 suppression. Oncogene. 2013;32:422–30.
19. Christofk HR, Vander Heiden MG, Harris MH, Ramanathan A, Gerszten RE, Wei R, Fleming MD, Schreiber SL, Cantley LC. The M2 splice isoform of pyruvate kinase is important for cancer metabolism and tumour growth. Nature. 2008;452:230–3.
20. Chang H, Xu Q, Li J, Li M, Zhang Z, Ma H, Yang X. Lactate secreted by PKM2 upregulation promotes Galectin-9-mediated immunosuppression via inhibiting NF-κB pathway in HNSCC. Cell Death Dis. 2021;12:725.
21. Qin X, Du Y, Chen X, Li W, Zhang J, Yang J. Activation of Akt protects cancer cells from growth inhibition induced by PKM2 knockdown. Cell Biosci. 2014;4:20.
22. Zhang X, Chen B, Wu J, Sha J, Yang B, Zhu J, Sun J, Hartung J, Bao E. Aspirin enhances the protection of Hsp90 from heat-stressed injury in cardiac microvascular endothelial cells through PI3K-Akt and PKM2 pathways. Cells. 2020;9:243.
23. Shen Q, Han Y, Wu K, He Y, Jiang X, Liu P, Xia C, Xiong Q, Liu R, Chen Q, Zhang Y, Zhao S, Yang C, Chen Y. MrgprF acts as a tumor suppressor in cutaneous melanoma by restraining PI3K/Akt signaling. Signal Transduct Target Ther. 2022;7:147.
24. Yang L, Dan HC, Sun M, Liu Q, Sun XM, Feldman RI, Hamilton AD, Polokoff M, Nicosia SV, Herlyn M, Sebti SM, Cheng JQ. Akt/protein kinase B signaling inhibitor-2, a selective small molecule inhibitor of Akt signaling with antitumor activity in cancer cells overexpressing Akt. Can Res. 2004;64:4394–9.
25. Martin SP, Fako V, Dang H, Dominguez DA, Khatib S, Ma L, Wang H, Zheng W, Wang XW. PKM2 inhibition may reverse therapeutic resistance to transarterial chemoembolization in hepatocellular carcinoma. J Exp Clin Cancer Res CR. 2020;39:99.
26. Yi Z, Wu Y, Zhang W, Wang T, Gong J, Cheng Y, Miao C. Activator-mediated pyruvate kinase M2 activation contributes to endotoxin tolerance by promoting mitochondrial biogenesis. Front Immunol. 2020;11:595316.
27. Kim E, Nam J, Chang W, Zulfugarov IS, Okhlopkova ZM, Olennikov D, Chirikova NK, Kim SW. Angelica gigas Nakai and Decursin downregulate Myc expression to promote cell death in B-cell lymphoma. Sci Rep. 2018;8:10590.
28. Watanabe Y, Taguchi K, Tanaka M. Ubiquitin, autophagy and neurodegenerative diseases. Cells. 2020;9:2022.
29. Rahman MA, Saikat ASM, Rahman MS, Islam M, Parvez MAK, Kim B. Recent update and drug target in molecular and pharmacological insights into autophagy modulation in cancer treatment and future progress. Cells. 2023;12:458.
30. Li T, Han J, Jia L, Hu X, Chen L, Wang Y. PKM2 coordinates glycolysis with mitochondrial fusion and oxidative phosphorylation. Protein Cell. 2019;10:583–94.
31. Niu D, Luo T, Wang H, Xia Y, Xie Z. Lactic acid in tumor invasion. Clin Chim Acta. 2021;522:61–9.
32. Zhang X, Zhang W, Wang Z, Zheng N, Yuan F, Li B, Li X, Deng L, Lin M, Chen X, Zhang M. Enhanced glycolysis in granulosa cells promotes the activation of primordial follicles through mTOR signaling. Cell Death Dis. 2022;13:87.
33. Hu R, Huffman KE, Chu M, Zhang Y, Minna JD, Yu Y. Quantitative secretomic analysis identifies extracellular protein factors that modulate the metastatic phenotype of non-small cell lung cancer. J Proteome Res. 2016;15:477–86.
34. Hong W, Guo F, Yang M, Xu D, Zhuang Z, Niu B, Bai Q, Li X. Hydroxysteroid sulfotransferase 2B1 affects gastric epithelial function and carcinogenesis induced by a carcinogenic agent. Lipids Health Dis. 2019;18:203.
35. Li Z, Li MY, Wang LL, Li L, Chen QY, Zhu YH, Li Y, Qin YR, Guan XY. The promoter hypermethylation of SULT2B1 accelerates esophagus tumorigenesis via downregulated PER1. Thoracic cancer. 2021;12:3370–9.
36. Hume S, Grou CP, Lascaux P, D'Angiolella V, Legrand AJ, Ramadan K, Dianov GL. The NUCKS1-SKP2-p21/p27 axis controls S phase entry. Nat Commun. 2021;12:6959.
37. Glaviano A, Foo ASC, Lam HY, Yap KCH, Jacot W, Jones RH, Eng H, Nair MG, Makvandi P, Geoerger B, Kulke MH, Baird RD, Prabhu JS, Carbone D, Pecoraro C, Teh DBL, Sethi G, Cavalieri V, Lin KH, Javidi-Sharifi NR, Toska E, Davids MS, Brown JR, Diana P, Stebbing J, Fruman DA, Kumar AP. PI3K/AKT/mTOR signaling transduction pathway and targeted therapies in cancer. Mol Cancer. 2023;22:138.
38. Wadhwa B, Makhdoomi U, Vishwakarma R, Malik F. Protein kinase B: emerging mechanisms of isoform-specific regulation of cellular signaling in cancer. Anticancer Drugs. 2017;28:569–80.
39. Chen QY, Costa M. PI3K/Akt/mTOR signaling pathway and the biphasic effect of arsenic in carcinogenesis. Mol Pharmacol. 2018;94:784–92.
40. Bhaskar PT, Hay N. The two TORCs and Akt. Dev Cell. 2007;12:487–502.
41. Celik A, Orfany A, Dearling J, Del Nido PJ, McCully JD, Bakar-Ates F. Mitochondrial transplantation: effects on chemotherapy in prostate and ovarian cancer cells in vitro and in vivo. Biomed Pharmacother Biomed Pharmacother. 2023;161:114524.
42. Fan XG, Pei SY, Zhou D, Zhou PC, Huang Y, Hu XW, Li T, Wang Y, Huang ZB, Li N. Melittin ameliorates inflammation in mouse acute liver failure via inhibition of PKM2-mediated Warburg effect. Acta Pharmacol Sin. 2021;42:1256–66.

43. Park YS, Kim DJ, Koo H, Jang SH, You YM, Cho JH, Yang SJ, Yu ES, Jung Y, Lee DC, Kim JA, Park ZY, Park KC, Yeom YI. AKT-induced PKM2 phosphorylation signals for IGF-1-stimulated cancer cell growth. Oncotarget. 2016;7:48155–67.

## Publisher's Note